Atmos. Chem. Phys. Discuss., 9, 26881–26924, 2009
www.atmos-chem-phys-discuss.net/9/26881/2009/

Atmospheric Chemistry and Physics Discussions

This discussion paper is/has been under review for the journal Atmospheric Chemistry and Physics (ACP). Please refer to the corresponding final paper in ACP if available.

A comparison of dry and wet season aerosol number fluxes over the Amazon rain forest

L. Ahlm[1], E. D. Nilsson[1], R. Krejci[1], E. M. Mårtensson[1], M. Vogt[1], and P. Artaxo[2]

[1]Department of Applied Environmental Science, Stockholm University, Stockholm, Sweden
[2]Institute of Physics, University of São Paulo, São Paulo, Brazil

Received: 5 November 2009 – Accepted: 3 December 2009 – Published: 15 December 2009

Correspondence to: L. Ahlm (lars.ahlm@itm.su.se)

Published by Copernicus Publications on behalf of the European Geosciences Union.

Abstract

Vertical number fluxes of aerosol particles and vertical fluxes of CO_2 were measured with the eddy covariance method at the top of a 53 m high tower in the Amazon rain forest as part of the LBA (The Large Scale Biosphere Atmosphere Experiment in Amazonia) experiment. The observed aerosol number fluxes included particles with sizes down to 10 nm in diameter. The measurements were carried out during the wet and dry season in 2008. In this study focus is on the dry season aerosol fluxes, with significant influence from biomass burning, and these are compared with aerosol fluxes measured during the wet season. The primary goal is to quantify the dry deposition sink and to investigate whether particle deposition velocities change when going from the clean wet season into the more polluted dry season. Furthermore, it is tested whether the rain forest is always a net sink of particles in terms of number concentrations, or if particle emission from the surface under certain circumstances may dominate over the dry deposition sink.

The particle deposition velocity v_d increased linearly with increasing friction velocity in both seasons and the relations are described by $v_{dd}=(2.7u_*-0.2)\times10^{-3}$ (dry season) and $v_{dw}=2.5u_*\times10^{-3}$ (wet season), where u_* is the friction velocity. The fact that the two relations are very similar to each other indicates that the seasonal change in aerosol number size distribution is not enough for causing any significant change in deposition velocity. In general, particle deposition velocities in this study are low compared to studies over boreal forests. The reason is probably domination of accumulation mode particles in the Amazon boundary layer, both in the dry and wet season, and low wind speeds in the tropics compared to the midlatitudes.

Net particle deposition fluxes prevailed in daytime in both seasons and the deposition flux was considerably larger in the dry season due to the much higher dry season particle concentration. In the dry season, nocturnal particle fluxes behaved very similar to the nocturnal CO_2 fluxes. Throughout the night, the measured particle flux at the top of the tower was close to zero, but early in the morning there was an upward particle

ACPD

9, 26881–26924, 2009

flux peak that is not likely a result of entrainment or local pollution. It is possible that these morning upward particle fluxes are associated with emission of natural biogenic particles from the rain forest. Emitted particles may be stored within the canopy during stable conditions at nighttime, similarly to CO_2, and being released from the canopy when conditions become more turbulent in the morning.

1 Introduction

The Amazonian forest is the largest tropical forest on Earth. During the wet season, the atmospheric boundary layer over the Amazon is relatively clean with low aerosol number concentrations (Artaxo et al., 2002; Martin et al., 2009; Zhou et al., 2002). In the dry season, however, when biomass burning is no longer suppressed by intense precipitation, aerosol concentrations are considerably higher and the aerosol population is dominated by anthropogenic particles (Andreae et al., 1988; Artaxo et al., 1998; Bowman et al., 2009). Elevated particle concentrations in the dry season influence climate directly through increased scattering of incoming solar radiation which in turn may affect the photosynthetic rate and thereby the regional carbon balance (Oliveira et al., 2007). Additionally, biomass burning particles are efficient cloud condensation nuclei (CCN) and therefore influence the formation of clouds and precipitation (Andreae et al., 2004; Gunthe et al., 2009; Koren et al., 2008). Moreover, absorption of solar radiation by smoke particles may lower the relative humidity and increase temperature in the absorbing layer, thereby reducing cloudiness and changing the atmospheric stability profile (Ackerman et al., 2000), which in turn affects turbulent fluxes of heat, moisture and even aerosol particles. Because of the intense convective activity over the rain forest, often associated with the Intertropical Convergence Zone (ITCZ), natural and anthropogenic aerosols can be uplifted to higher altitudes and be transported far away from the tropics and in this manner also have a global impact on climate (Andreae et al., 2001).

ACPD
9, 26881–26924, 2009

In order to fully represent the impact from biomass burning on regional and global climate, it is important to reduce the uncertainties in particle number emission factors from biomass burning (Andreae and Merlet, 2001; Lohmann et al., 2007), but also to understand the processes controlling removal of aerosols from the atmosphere. The most important deposition processes are wet and dry deposition. The efficiency of dry deposition is highly dependent on particle size (Slinn et al., 1982). Particle emission from biomass burning is dominated by accumulation mode particles (Artaxo et al., 1994; Reid et al., 2005), for which there is no efficient dry deposition mechanism.

Rissler et al. (2004) investigated the surface aerosol size distribution in Rondônia in the southwestern part of the Amazon, and found that the size distribution was dominated by an Aitken and an accumulation mode both in the dry and wet season. Rissler et al. (2006) observed increasing geometrical diameter of the two modes with increasing influence from biomass burning in a study in Balbina, located 125 km northeast of Manaus. In the same study, particle concentrations were elevated during an aged biomass burning period compared to the clean background air mass by nearly a factor of 2 in the Aitken mode size range, and 4–5 times in the accumulation mode size range. The higher percentage of accumulation mode particles in the dry season could have an impact on the dry deposition velocities. By measuring vertical aerosol number fluxes, the dry deposition sink can be quantified. Furthermore, vertical particle fluxes reveal whether the rain forest always acts as a net particle sink, or if it under certain conditions may be a net particle source. Natural biogenic particles are present in both the dry and wet season (Graham et al., 2003), and are a significant fraction of the aerosol mass, with a strong dominance of coarse mode particles (Artaxo and Hansson, 2005). There is a strong diurnal variability in biogenic particle concentrations due to change in emissions processes, deposition and meteorological forcings (Graham et al., 2003).

To our knowledge, Ahlm et al. (2009) contains the first peer-review published results ever on eddy covariance aerosol particle fluxes over the Amazon rain forest. That study was based on wet season measurements in the Cuieiras Ecological Reserve close to Manaus in the northern part of the Amazon rain forest. The study showed that net

ACPD
9, 26881–26924, 2009

particle fluxes pointed downward even in the absolute cleanest conditions. This was an indication that secondary aerosol particles formed above the measurement tower may dominate the background aerosol number population in the Amazon boundary layer, and that the contribution from primary aerosol emission may be low.

In this study, focus is on the dry season particle fluxes, with larger impact from anthropogenic sources, and these fluxes are compared with particle fluxes measured in the wet season. The goal is to quantify the dry deposition sink and also to investigate whether the particle deposition velocities change during transition from the wet season into the dry season. Furthermore, it is tested whether the rain forest is a net sink of particles also in the dry season, or if particle emission from the surface under certain circumstances may dominate over the dry deposition sink. This Brazilian-Swedish project AMAFLUX (Amazonian Biosphere-Atmosphere Aerosol Fluxes in view of their potential control of cloud properties and climate) was carried out as a part of the larger international project LBA (The Large Scale Biosphere Atmosphere Experiment in Amazonia) and the measurement were performed in 2008.

2 Method

2.1 Site description

The measurements were carried out at the top of the 53 meter high tower K34 in the Reserva Biológica do Cuieiras (2°35.37′ S, 60°06.92′ W), approximately 60 km NNW of Manaus, Brazil. The tower is a research facility operated by INPA (The Brazilian National Institute for Research in Amazonia). The canopy height in the Cuieiras Reserve is between 30 and 35 m (Kruijt et al., 2000). Figure 1 shows the location of the measurement site. A more detailed description of this site can be found in Ahlm et al. (2009).

ACPD
9, 26881–26924, 2009

2.2 Eddy covariance measurements

The vertical aerosol number flux was calculated with the eddy covariance technique. The aerosol number concentration N and the vertical wind speed w can be divided into means and fluctuations from the mean, $N=\overline{N}+N'$ and $w=\overline{w}+w'$. By following the Reynold's averaging rules, it can be shown that $\overline{Nw}=\overline{N}\overline{w}+\overline{N'w'}$ where $\overline{N}\overline{w}$ is the vertical advective flux and $\overline{N'w'}$ is the vertical turbulent flux. When the flux measurements are performed within the surface layer, vertical advection is assumed to be a result of the terrain and therefore the coordinate system is rotated in order to obtain zero vertical advection. Then the total vertical flux becomes equal to the turbulent vertical flux.

Campos et al. (2009) investigated turbulent time scales at K34 by using multiresolution decomposition technique. They found that the average time scale was below 200 s at nighttime and below 1200 s in daytime for CO_2 and energy fluxes. Hence, it is preferable to use short time scales when rotating and de-trending fluxes measured within the nocturnal boundary layer to obtain as stationary conditions as possible and thereby minimizing the uncertainty of the flux. However, in daytime it is necessary to use longer time scales to include the largest eddies within the mixed layer. Even though the daytime turbulence time scale is on average below 1200 s, eddies with considerably lower frequencies have been observed to contribute to energy fluxes over the Amazon (Finnigan et al., 2003). However, the variability of the aerosol number concentration is much larger than the variability of temperature and water vapor (or even CO_2). To de-trend particle concentrations and calculate the particle fluxes over very long time scales would often produce large errors and increase the uncertainty of the particle flux.

For this study the vertical aerosol flux $\overline{N'w'}$ was calculated and linearly de-trended over three different time scales to make it possible to investigate both daytime and nighttime fluxes. The chosen time scales were 30, 10 and 3 min long. The aerosol data was shifted in relation to the wind data to correct for the time lag in the sampling line (calculated from the maximum correlation). Turbulent fluxes of momentum, energy

ACPD
9, 26881–26924, 2009

and CO_2 were calculated in a similar way, but only over time scales of 30 min since the magnitude of these fluxes is not the main objective of this study.

2.3 Instrumentation

2.3.1 Flux measurements

The 3-D wind components and temperature were measured with a Gill Windmaster ultrasonic anemometer, and logged at 20 Hz. To measure the total aerosol number concentration (particle diameter D_p>10 nm) we used a Condensation Particle Counter (CPC), model TSI 3010, which was logged at 1 Hz. The aerosol was sampled just beneath the sonic head through a 4 m long 1/4-inch stainless steel sampling line. The sampling flow through the CPC was 1.08 l min^{-1}.

Concentrations of CO_2 and H_2O were measured by a Li-7500 Open Path Analyzer. The Licor was logged both as digital RS232 signals through an EDG-4508 gateway and as analog signals through the Gill windmaster auxiliary input channels, in both cases at 20 Hz.

The most frequent technical problem encountered during the campaign was condensation of water vapor inside the CPC saturator. Therefore the CPC reservoir had to be drained and thereafter filled with new butanol more or less every day. This problem was related to the high water content of the air.

2.3.2 Additional data used during data analysis

Mass concentration of equivalent black carbon (BC_e) was provided by São Paulo University using a Multi-Angle Absorption Photometer (MAAP). This measurement derives the concentration of BC_e from the determination of light absorption at a wavelength of 670 nm using an empirical mass absorption efficiency of 6.5 m^2 g^{-1}. Because of uncertainties regarding the appropriate value of the mass absorption efficiency and the possibility of contributions from light-absorbing organic aerosols, we choose the term

ACPD
9, 26881–26924, 2009

BC_e to reflect the operational definition of this measurement (Andreae and Gelencsér, 2006). BC_e was measured at a container close to the house at the center of the research station, approximately 2 km north of K34.

Additional meteorological parameters (temperature, relative humidity, rain amount and photosynthetic active radiation) were measured at the K34 tower and provided by INPA. These were logged on a Campbell CR-10 (Campbell Scientific UK) data logger with a sampling interval of 30 s and stored as either 10 or 30 min averages.

2.4 Flux corrections

2.4.1 Effects of limited instrumental frequency response

The underestimation of the particle flux due to limited time response of the CPC depends on the frequency of the turbulence. It can approximately be determined by the observation level z (53 m), mean horizontal wind speed $\overline{U}$ and stratification z/L, where L is the Obukhov length. The underestimation in the flux can be estimated (Buzorius et al., 2003) as

$$\frac{F_m}{F} = \frac{1}{1+(2\pi n_m \tau_c \overline{U}/z)^{\alpha}} \quad (1)$$

with α=1 for $z/L>0$ (stable stratification) and α=7/8 for $z/L \leq 0$ (neutral and unstable stratification). The normalized frequency, n_m, equals 0.085 for $z/L \leq 0$ and

$$n_m = 2.0 - \frac{1.915}{1+0.5\frac{z}{L}} \quad \text{for} \quad z/L > 0. \quad (2)$$

The frequency first order response time constant τ_c of the TSI 3010 has been estimated to 0.8 s (Doebelin, 1990). However, in this study the particle concentration was measured at a frequency of 1 Hz and therefore a value of 1 s on τ_c has been used in Eq. (1).

ACPD
9, 26881–26924, 2009

All aerosol fluxes presented in this work have been corrected according to Eqs. (1) and (2). The correction when using these equations was on average 13% of the measured net aerosol flux in both the dry and wet season.

2.4.2 Webb-correction

The assumption behind the Webb correction is that the vertical mass flux of dry air is zero:

$$\overline{w\rho_a} = 0$$

where w is the vertical wind speed and ρ_a is the density of dry air. At least in a non-stable surface layer, ascending air on average will be warmer and contain more water vapor (thereby having lower density) than descending air. Therefore the mean of the vertical wind speed $\overline{w}$ usually must be positive for the mass flux of dry air to be zero. A positive $\overline{w}$ produces a positive vertical advection term that must be added to the measured turbulent flux. This correction is known as the Webb correction (Webb, 1980) and the total flux is

$$F = \overline{w'c'} + 1.61\frac{\overline{w'\rho_v'}}{\overline{\rho_a}} + (1 + 1.61\overline{q})\frac{\overline{w'T'}}{\overline{T}}\overline{c} \quad (3)$$

where ρ_v' is fluctuation in density of water vapor, $\overline{q}$ is the averaged specific humidity and $\overline{T}$ is the average temperature, T' the fluctuating part of the temperature, $\overline{c}$ is the average and c' the fluctuating part of the concentration of the substance. In this study, the Webb correction has been applied to the CO_2 and the latent heat flux. The Webb correction at noon (when energy fluxes are at maximum) reduced the net downward CO_2 flux with about 45% in the dry season and 25% in the wet season. The corresponding increase in latent heat flux was 13% and 9% in the dry and wet season, respectively.

The situation is more complicated for particle fluxes. Temperature fluctuations are dampened in a tubing of several meters (Rannik et al., 1997). Probably even more

ACPD
9, 26881–26924, 2009

important, inside the CPC the air is both heated and cooled, as part of the detection process, before the flow rate is set by the critical orifice inside the CPC. Concerning water vapor, a fraction of the water vapor entering the CPC inlet is deposited in the butanol in the CPC reservoir before the particles are being counted and the flow rate is set inside the CPC. It is hard to estimate what fraction of water vapor flowing into the CPC that is trapped there, but during this campaign it seems to have been a significant amount. Therefore, no Webb correction was applied to the particle fluxes.

2.5 Error treatment

Following Buzorius et al. (2003), the uncertainty in the flux due to discrete counting can be expressed as

$$\delta(N'w') = \frac{\sigma_w \overline{N}}{\sqrt{\overline{N} Q \Delta t}} \tag{4}$$

where σ_w is the standard deviation of the vertical wind, $\overline{N}$ is the aerosol number concentration averaged over the sampling period Δt (in our case 30, 10 and 3 min) and Q is the sampling volume flow rate through the particle counter. When considering relative errors, high turbulence and number concentrations usually correspond to high aerosol number fluxes, so the relative error may actually decrease with increasing $\overline{N}$ and σ_w, and vice versa. The average uncertainty in particle flux (calculated over 30 min) due to discrete counting was in this study 2.2% in the dry season and 3.1% in the wet season. There are of course other sources of uncertainty in aerosol flux quantification than but these errors are more difficult to quantify.

ACPD
9, 26881–26924, 2009

3 Results and discussion

The measurements included in this study were performed between 12 March and 18 May (wet season) and between 15 July and 12 August 2008 (dry season). Concerning the wet season CPC measurements, 37% of the data had to be removed because of technical problems, mainly linked to water uptake in the CPC butanol reservoir. The corresponding loss of data from the dry season was only 8%.

Of the CO_2 and H_2O measurements, 15% of the data were rejected from the wet season data and 19% from the dry season data, primarily due to problems with electricity or computer software and spikes in raw data during rainfall.

Meteorological and BC_e measurements ran more or less continuously during the period. The concentrations of the different compounds have not been converted to STP (standard temperature and pressure) conditions. The reason for this is that the exact temperature when counting the particles inside the CPC was not well known. The condensation temperature inside the CPC was logged but the air will have a somewhat higher temperature when the particles are being counted and the sampling flow rate is set. An estimation of this temperature would produce new errors. For consistency, neither the concentrations of the other compounds have been converted to STP and thereby represent ambient conditions.

3.1 Average conditions during the campaign

Tables 1 and 2 show the average meteorological conditions, concentrations and fluxes during the two measurement periods, the dry and wet season, respectively. The flux parameters are defined as positive when the flux is upward and negative when the flux is downward.

The difference in BC_e concentration between the dry and wet season (Tables 1 and 2) in this study shows the impact of biomass burning emissions in the dry season at the Cuieiras Reserve. The mean dry season BC_e concentration was $259 \pm 115\,ng\,m^{-3}$ and the corresponding concentration in the wet season was

ACPD
9, 26881–26924, 2009

$80 \pm 45\,\mathrm{ng\,m^{-3}}$ (mean±standard deviation). The other parameters will be discussed closer in next section.

3.2 Diurnal cycles of meteorological parameters

This section deals with the average diurnal cycles of meteorological parameters. These are important when later interpreting the vertical aerosol number fluxes. The diurnal cycles (Fig. 2a–j) are shown as medians of half-hour mean values. The reason for choosing median cycles instead of mean cycles is to reduce the weight of extreme values and instead show what is happening more frequently. The only exception is the diurnal cycle of rainfall (Fig. 2j), where it makes more sense to use mean cycle, since the median rain amount is zero for a large fraction of the half hour intervals forming the diurnal cycle.

The sunrise was around 06:00 LT (local time) and the sunset at 18:00 LT, which can be seen in the curve showing Photosynthetic Active Radiation (PAR) (Fig. 2a). The PAR is higher in the dry season than in the wet season, due to less cloudiness in the dry season. The curves for sensible (Fig. 2b) and latent (Fig. 2c) heat fluxes are rather well correlated with the PAR, and these fluxes are larger in the dry season because the incoming solar radiation (as well as the PAR) then is higher. Also the temperature (Fig. 2d) is higher in the dry season with the largest difference between the two seasons prevailing during afternoon.

As was discussed in Ahlm et al. (2009), much information of the diurnal cycle of the boundary layer can be revealed by investigating the diurnal cycle of water vapor concentration (Fig. 2e). In the morning between 06:00 LT and 09:00 LT, before the nocturnal inversion has been defeated, the mixed layer grows very slowly and the water vapor from evapotranspiration is trapped in a thin mixed layer connected to the surface. However, after the nocturnal inversion has been defeated and resistance to further growth is much lower (Stull et al., 1988), the mixed layer grows fast and entrainment of drier air from above then dominates over evapotranspiration. This results in decreasing

ACPD
9, 26881–26924, 2009

water vapor concentration despite enhancing evapotranspiration with increasing PAR. In Fig. 2e, it is obvious that the switch from increasing to decreasing water vapor concentration occurs around 09:00 LT both in the dry and in the wet season. Hence, it seems that the burning off of the nocturnal inversion occurs at approximately the same time in the two seasons. The water vapor concentration is generally higher in the dry season than in the wet season even though the relative humidity (Fig. 2f) is higher in the wet season (due to lower temperature in the wet season).

Figure 2g reveals the differences in stability, L^{-1}, between the two seasons, where L is the Obukhov length. In daytime, an unstable convective boundary layer is present both in the dry and wet season with similar values on L^{-1}. However, the difference in stability between the two seasons is clearly visible at nighttime. A typical nocturnal stable boundary layer forms one or two hours before sunset in the dry season (also seen as negative sensible heat flux in Fig. 2b) and at nighttime the stratification is highly stable. The nocturnal boundary layer reaches on average a final depth of 80–180 m (Garstang et al., 1990). However, this stable nocturnal layer is less pronounced in the wet season with sometimes unstable conditions also at nighttime, seen in higher nighttime wet season friction velocities (Fig. 2i) and also higher nighttime wet season rain amounts (Fig. 2j). The daytime friction velocity is often higher in the dry season than in the wet season, probably to a large extent due to higher daytime wind speeds (Fig. 2h) in the dry season.

3.3 Diurnal cycles of concentration and flux of CO_2

In this section, diurnal cycles of CO_2 concentration and flux are analyzed. The primary reason for investigating also fluxes of CO_2 in this study, is that the diurnal cycles of the CO_2 and the particle flux show some similarities that will be a help when interpreting the particle fluxes in detail in Sect. 3.4.

The CO_2 concentration and flux have a very distinct diurnal cycle (Fig. 3). In daytime there is an uptake of CO_2 by the forest (downward fluxes) and the atmospheric CO_2 concentration consequently decreases. During evening and nighttime, when there is

ACPD
9, 26881–26924, 2009

no photosynthetic active radiation and only CO_2 emission (upward fluxes), instead the CO_2 concentration increases. In Fig. 3, it is obvious that the daytime uptake of CO_2 is slightly higher in the wet season (Fig. 3b) than in the dry season (Fig. 3a), which also was observed by Araújo et al. (2008). An interesting difference between the two seasons is the peak in upward flux, between 07:00 LT and 08:00 LT, apparent in the dry season curve but not in the wet season curve. In the same time interval, the dry season concentration rapidly increases followed by a peak in concentration, whereas the wet season concentration curve has a more continuous shape. Malhi et al. (1998) noticed that on calm nights with stable stratification, most of the respired CO_2 is stored within the forest canopy and released in the morning when conditions become more turbulent, while during less stable nights most of the CO_2 is released intermittently throughout the night. They found the threshold friction velocity, separating the two cases, to be 0.1 $m\,s^{-1}$. This explains the patterns seen in Fig. 3. In the wet season, nighttime friction velocities (Fig. 2i) are close to or above 0.1 $m\,s^{-1}$ and the CO_2 flux points steady upward throughout the night, although varying in magnitude. In the dry season, however, nighttime friction velocities are considerably lower and the nighttime CO_2 flux is therefore close to zero with a following large emission peak at 07:00–08:00 LT when conditions become more turbulent.

It is since long known that respiration is often underestimated by nighttime eddy covariance measurements over forest canopies and that this underestimation is most significant in calm nights with low wind speeds (Goulden et al., 1996), a very frequent situation. At nighttime, the canopy layer becomes decoupled from the atmosphere above. The airflow above the canopy is then synoptically driven, while the airflow within the canopy moves downslope (Aubinet et al., 2003; Marcolla el al., 2005). There is growing evidence that nighttime advection caused by these drainage flows is the root cause of the failure to capture the respiration flux in stable conditions at nighttime (Finnigan et al., 2008).

Araújo et al. (2008) investigated the nocturnal CO_2 concentration field in the heterogeneous terrain of the Cuieiras Reserve of valleys and slopes and found that,

ACPD
9, 26881–26924, 2009

particularly during stable nights, large amounts of CO_2 were transported downslope by drainage flows from the K34 plateau and being accumulated in valleys. This is useful information when later moving to the diurnal cycle of the vertical particle flux in Sect. 3.4.2.

3.4 Aerosol number fluxes and concentrations

3.4.1 Concentrations of particles in the dry and wet season

The mean aerosol number concentration and standard deviation in the dry and wet season were 1513±721 cm^{-3} and 682±780 cm^{-3}, respectively (Tables 1 and 2). The corresponding median values were 1352 cm^{-3} and 466 cm^{-3}. Hence, the mean particle concentration was roughly two times higher in the dry season than in the wet season while the median particle concentration was approximately three times higher in the dry season. This means that the dry season particle concentration most of the time was three times higher than the wet season concentration, but some occasionally high peaks in wet season particle concentration brings the mean concentrations in the two seasons closer to each other compared to the median concentrations. This can also be seen in the higher standard deviation in the wet season aerosol number concentration.

The difference in particle concentration between the two seasons is much less pronounced in this study than in other studies in Rondônia in the southwestern part of the Amazon rain forest (Rissler et al., 2006). The reason for this is that the Cueiras Reserve is located in an area of pristine rain forest where the direct influence of biomass burning is much lower than in Rondônia or other locations in the southern part of the Amazon rain forest. Even in the dry season, impact of biomass burning emissions is not very high at the Cuieiras Reserve, but can be observed most of the time.

ACPD
9, 26881–26924, 2009

3.4.2 Dependence on wind direction

Figure 4 shows the dependence on wind direction for the aerosol number concentration in the dry (Fig. 4a) and wet (Fig. 4b) season and for the aerosol number flux in the dry (Fig. 4c) and wet (Fig. 4d) season. The dry season aerosol number concentration peaks when the wind direction is between 170–200 degrees, which represents advection of air with large influence from biomass burning in the southern part of the Amazon rain forest. The wet season aerosol concentration peaks when winds are southeasterly which represents advection from the city Manaus. Hence, it seems that Manaus is the dominant source of air pollution in the wet season but not in the dry season.

In Fig. 4c and d it is obvious that downward particle fluxes dominate both in the dry and wet season and deposition fluxes are considerably larger in the dry season when particle concentrations are much higher. The net upward particle flux in the wet season, associated with northwesterly winds (Fig. 4d), is likely a result of local pollution from the diesel generator (Ahlm et al., 2009) located within the research station (Fig. 1).

3.4.3 Diurnal cycles of the vertical particle flux

In this section, median diurnal cycles of the particle flux in the two seasons are investigated. Main focus is on the dry season particle flux and it is compared with the wet season particle flux. In order to exclude any possible impact from the diesel generator and the house on the particle fluxes at K34, time periods with mean wind directions between 310 and 20 degrees have been excluded in the calculations of these diurnal cycles. In addition, time periods of rainfall have been ignored to simplify interpretation of the fluxes.

Figure 5 shows median diurnal cycles of the vertical particle flux in the dry and wet season, with 25 and 75 percentiles (Fig. 5a) and with error bars representing counting errors (Fig. 5b). These fluxes have been calculated and de-trended over periods of 30 min. The particle flux is in general small at nighttime but larger in daytime when the turbulence intensity is much higher (Fig. 2i). In daytime, the median particle flux points

ACPD
9, 26881–26924, 2009

downward both in the dry and wet season, indicating net deposition. The dry season daytime deposition flux is significantly larger in the dry season than in the wet season. A larger deposition flux in the dry season is of course expected since anthropogenic impact on the aerosol population is significantly higher in the dry season, even though also the wet season particle flux contains some influence from anthropogenic sources.

The maximum deposition flux occurs around noon and is $\sim 1.0 \times 10^6$ particles m^{-2} s^{-1} in the dry season and $\sim 0.3 \times 10^6$ particles m^{-2} s^{-1} in the wet season (Fig. 5). An approximate impact of these deposition fluxes on the particle concentration for each season can be estimated by using the median aerosol number concentration in Tables 1 and 2 for each season and assuming a maximum daytime mixed layer depth of 1100 m in the dry season and 1000 m in the wet season (Fisch et al., 2004). Then the deposition fluxes on average decrease the particle concentration around noon with 3.3 particles per cm^3 per hour in the dry season and 1.1 particles per cm^3 per hour in the wet season. The percentage loss is actually the same in both seasons, 0.24% of the total particle population is deposited per hour at noon.

3.4.4 Upward particle fluxes

The wet season particle flux was analyzed in detail in Ahlm et al. (2009). There it was concluded that the upward flux peak between 10:00 and 11:00 LT most likely is a result of entrainment of cleaner air from above during fast mixed layer growth after the nocturnal inversion has been defeated. The dry season curve, however, has a quite large upward flux peak between 07:00 and 08:00 LT. At this time, the nocturnal inversion has not been defeated according to the discussion of the diurnal cycle of water vapor concentration in Sect. 3.2. The mixed layer can therefore be expected to grow very slowly at this time, which means that the upward flux peak is not likely a result of entrainment fluxes. Furthermore, the upward particle fluxes appear already 06:00 LT in the morning (even though the peak is a bit later) which further reduces the possibility of entrainment fluxes being a valid explanation. The mixed layer is still thin this early in the morning which means that the associated turbulent time scales are short. Therefore

ACPD
9, 26881–26924, 2009

fluxes calculated over 30 min (Fig. 5) are associated with large uncertainties. However, the upward flux peak is apparent also when shorter time scales (10 and 3 min) are used for calculating the dry season flux (Fig. 6), and therefore these early morning upward particle fluxes seem reliable.

It is interesting to compare the median dry season diurnal cycle of the particle flux (Fig. 5) with the dry season diurnal cycle of CO_2 flux in Fig. 3. Obviously the peaks of the morning upward flux of particles and CO_2 occur at the same time. The peak in upward CO_2 flux in the morning was explained by release of CO_2, that has been stored within the canopy during the night, when conditions become more turbulent in the morning (Sect. 3.3). It is possible that also particles are being emitted from the forest throughout the whole night but stay confined within the canopy until turbulence starts increasing after sunrise, which mixes up these particles so an upward flux appears at the altitude where the measurements are made, at the top of the tower K34. Hence, while net particle deposition dominates at nighttime in the wet season, net particle emission may dominate at nighttime, or at least in the early morning, in the dry season. These dry season emission fluxes are not likely a result of local pollution, since the wind sector associated with advection from the diesel generator and the house have been excluded when calculating the diurnal cycles. Instead these upward fluxes actually may be a result of emission of natural biogenic particle from the forest.

In the case of CO_2, it is very clear that the morning peak in upward flux is due to emission, because the CO_2 concentration peaks at the same time. However, the median diurnal cycle of particle concentration (Fig. 7) shows a different behavior than the diurnal cycle of CO_2 concentration. From midnight and until morning, the particle concentration decreases. The particle concentration actually continues its decreasing trend from the night when the upward particle flux appears in the morning. However, an emission source of 0.5×10^6 particles m^{-2} s^{-1}, like the early morning median upward flux in Fig. 5, active during one hour would only increase the particle concentration with 18 particles per cm^3 in a ~100m thick boundary layer, which is only a little more than a one percent increase in particle concentration. The particle concentration in Fig. 7

ACPD
9, 26881–26924, 2009

shows a decreasing trend from midnight until 10:00 LT and the relatively small gain of particles from the emission flux in the morning is insignificant compared to the overall negative trend in concentration. Therefore, particle emission from the forest is still a possible explanation for the median upward flux around 08:00 LT, even though there is no peak in particle concentration at the same time.

Since nighttime respiration is known to be underestimated by eddy covariance measurements in tropical forests, also nighttime particle emission is then probably somewhat underestimated. Furthermore, it is also possible that nocturnal drainage flows transport particles away from the plateau where K34 is located to valleys in the surroundings. In the future, it would of course be interesting to investigate nocturnal horizontal particle gradients between plateaus and valleys, like Araújo et al. (2008) have made for CO_2, and possibly also try to quantify the nocturnal downslope advection of particles from the plateau of K34 like Tóta et al. (2008) have made for CO_2 as a tool for estimating the "missing flux".

The median diurnal cycle of the dry season particle flux in Fig. 5 shows dominating upward particle fluxes also in the evening from about 19:00 LT until 24:00 LT. However, when timescales of 10 and 3 min are used for calculating the fluxes (Fig. 6), the particle flux instead oscillates around zero at this time interval. Hence, it seems that the evening upward particle flux obtained by using time scales of 30 min is not reliable. However, as stated before, the peak in upward particle flux at 08:00 LT is present in the particle flux regardless of time scale used for flux calculation and de-trending. The emission flux in the morning therefore seems reliable.

The fact that net emission seems to prevail at nighttime in the dry season but not in the wet season is an indication that nocturnal emission of natural biogenic particles from the forest may be favored by dry conditions. However, the fact that the upward fluxes appear in the morning does not necessarily means that the emission source is lower in daytime than at nighttime. Particles emitted at nighttime may be stored in the canopy layer which is decoupled from the atmosphere in stable conditions. Artaxo and Hanssen (1985) and Guyon et al. (2003a,b), observed an increase

ACPD
9, 26881–26924, 2009

in phosphorus concentration during nighttime at the lower part of the canopy, and they attributed this enhancement to nighttime biogenic emissions of particles containing phosphorus. Hence, the upward flux in the early morning is then the flux of approximately all particles that have been emitted and stored under the canopy throughout the night. In daytime, when conditions are more turbulent, an emission of the same magnitude would generate upward fluxes that are more continuous and these emission fluxes would drown in the large daytime deposition flux.

3.4.5 Particle deposition velocities

The particle dry deposition velocity can be estimated from flux measurements by dividing the particle flux with the number concentration. The deposition velocity v_d is defined as

$$v_d = -\frac{F}{c} \tag{5}$$

where F is the particle number flux and c is the particle number concentration. Positive values on v_d represents net downward flux.

Figure 8 shows the median diurnal cycles of v_d both in the dry and wet season for fluxes calculated and de-trended over time scales of 30 min. v_d is low at nighttime but higher in daytime when conditions are more turbulent. There seems to be no significant difference in daytime particle deposition velocity between the dry and wet season. In both seasons, v_d peaks at approximately 1 mm s^{-1} in the middle of the day or early afternoon. At nighttime, the deposition velocities have different signs in the two seasons as a result of net deposition at nighttime in the wet season and net emission at nighttime in the dry season. To include periods of net upward fluxes when estimating deposition velocities, of course means that the deposition velocities are somewhat underestimated, because some of the upward fluxes point upward for a physical reason and not only because of random errors. However, to exclude all net upward fluxes would probably result in an even larger overestimation of the deposition velocity since a large fraction of the upward fluxes are only results of random errors.

ACPD
9, 26881–26924, 2009

In general, deposition velocities are low here compared to studies over boreal forests (Ruijgrok et al., 1997; Buzorius et al., 2000; Gaman et al., 2004; Pryor et al., 2007). Dominance of accumulation mode particles in Amazon boundary layer, both in the dry and wet season, is one explanation for these low values on v_d. Another important reason is the low wind speeds in the tropics compared to the midlatitudes. When considering the fact that wet deposition is a very important deposition process over tropical rain forests (as a result of the high rain amounts) and adding the low particle deposition velocities found in this study, it can be stated that the relative contribution of dry deposition to total deposition of particles is much lower in the continental tropics than in the continental midlatitudes. In this way, the continental tropics resemble many marine environments.

3.4.6 Dependence on friction velocity

Figure 9a shows the particle deposition velocity as a function of friction velocity. Obviously, the deposition velocity increases with increasing friction velocity in a linear way both in the dry and wet season. The relation in the dry season is described by

$$v_{dd} = (2.7u_* - 0.2) \times 10^{-3} \quad (6)$$

and in the wet season by

$$v_{dw} = 2.5u_* \times 10^{-3} \quad (7)$$

The deposition velocities are slightly higher in the wet season than in the dry season in Fig. 9a. However, when adding 25 and 75 percentiles (Fig. 9b), it becomes obvious that the difference in v_d between the dry and wet season is negligible compared to the variability in each season.

Most studies of dry deposition for particles have shown that the minimum deposition velocity is located at diameters around 0.1–0.3 µm (Zhang and Vet, 2006). For lower particle sizes, Brownian diffusion becomes more efficient and for larger sizes interception and impaction become increasingly important (Slinn, 1982).

ACPD
9, 26881–26924, 2009

As was mentioned in the introduction, during transition from the wet season into the dry season, the percentage of accumulation mode particles within the Amazon boundary layer has been observed to increase with a following percentage decrease of Aitken mode particles (Rissler et al., 2004). Rissler et al. (2006) observed increasing geometrical diameter of the two modes with increasing influence from biomass burning. In the wet period, the accumulation mode and the Aitken mode had geometrical mean diameters of 128 and 61 nm, and in the dry period the corresponding values were 190 and 92 nm. An additional nucleation mode was observed rather frequently centered at ~20nm, but with a lower number concentration. Zhou et al. (2002) reported geometrical diameters of 151 and 68 nm of the accumulation and the Aitken mode in the wet season in Balbina during the wet season. A smaller mode was only occasionally observed (centered at ~24nm) and this mode could almost exclusively be linked to local pollution. A change towards a somewhat higher percentage of particles in the accumulation mode in the dry season, observed by Rissler et al. (2004), will reduce the efficiency of dry deposition since the efficiency of Brownian diffusion decreases with increasing particle size. However, the very similar values in dry and wet season values on v_d obtained in this study (Fig. 9b) indicate that the change in size distribution between the wet and dry season is not enough to have a significant impact on the overall particle deposition velocity.

There is of course a possibility that the accumulation mode particles deposit more efficiently in the dry season, since they in this time period may be somewhat larger, which could make interception and impaction more efficient. This effect could counteract the effect of decreasing dry deposition due to lower percentage of Aitken mode particles in the dry season. Another factor that might have an influence is the seasonal variations in leaf area index (LAI). The LAI has been observed to increase during the dry season with as much as 25% from the annual mean (Myneni et al., 2007). A larger LAI means more area for particles to deposit on. Hence, a larger dry season LAI could increase the dry season particle deposition velocities, thereby also counteracting the effect of higher dry season percentage of accumulation mode particles. The difference

ACPD
9, 26881–26924, 2009

in impact of particle rebound in dry and wet conditions, respectively, is probably of less importance since particle bounce off primarily affects coarse particles, which are very low in numbers, and therefore do not have a large influence on particle fluxes measured with CPC.

3.4.7 Dependence on stability

Wesely et al. (1985) proposed the following relation for deposition of sulfate particles over grass:

$$v_{ds} = 0.002u_* \quad L \geq 0 \tag{8}$$

$$v_{ds} = 0.002u_*(1+(-300/L)^{2/3}) \quad L < 0 \tag{9}$$

where v_{ds} is the surface deposition velocity defined as

$$v_{ds} = \frac{1}{\frac{1}{v_d} - r_a} \tag{10}$$

where r_a is the aerodynamic resistance.

In this study, we have made a rough estimate of the aerodynamic resistance by using relations given in Seinfeld and Pandis et al. (1998) with assumed values on the roughness length and the displacement height as 1.8 m and 25.8 m, respectively (Harris et al., 2004). r_a is high at nighttime and low in daytime (Fig. 10a). In the time period 10:00–16:00 LT, r_a varies between 10 and 15 s m^{-1} in both the dry and wet season. Since the deposition velocity in the same time period varies between 0.5 and 1 mm s^{-1} (Fig. 8), it is obvious from Eq. (9) that $v_d \approx v_{ds}$ in daytime, and there is no need to convert v_d to v_{ds} for making a comparison with the Wesely relation in daytime conditions. It also seems preferable not to convert v_d to v_{ds} when not necessary, since the estimations of r_a in this study are only rough estimations, however, probably accurate enough to state that $v_d \approx v_{ds}$ in daytime.

ACPD
9, 26881–26924, 2009

Figure 10b shows how the ratio $\frac{v_d}{u_*}$ depends on L^{-1} for negative values on L^{-1} during both the dry and wet season. The reason for ignoring the stable case is that the dry season fluxes to a large extent point upward in the stable conditions prevailing at nighttime, thereby not providing much information of deposition rates in these conditions. However, a dominating part of the total dry deposition occurs in the unstable stratification prevailing in daytime (Fig. 5), and therefore the unstable case is by far the most important case. In Fig. 10b, only data collected between 12:00 LT and 16:00 LT are used, a time period when entrainment may be expected to have a relatively low impact on the aerosol flux. A curve describing the relation by Wesely et al. (1985) in Eq. (8) has been included as a comparison. It can be seen that the ratio $\frac{v_d}{u_*}$ on average slightly increases with decreasing stability in unstable conditions both in the dry and wet season. However, the dependence on stability is much lower than was observed by Wesely et al. (1985), and the error bars, showing 25 and 75 percentiles, reveal that the variability is large. The dependence on stability appears to have low variation between the two seasons.

4 Summary and conclusions

Aerosol number fluxes and CO_2 fluxes were measured with the eddy covariance method over the Amazon rain forest in 2008 in both the dry and wet season. The measurements were performed at the top of the 53 m high tower K34 in the Cuieiras Reserve, Manaus, Brazil. Aerosol number fluxes measured during the dry season, when the impact from biomass burning is high, are compared with fluxes measured in the much cleaner conditions prevailing in the wet season. The key results and main conclusions are:

– The median aerosol number concentration was 1352 cm^{-3} in the dry season and 466 cm^{-3} in the wet season.

ACPD
9, 26881–26924, 2009

- Particle deposition velocities peak around noon or in early afternoon at approximately 1 mm s^{-1} both in the dry and wet season. The daytime particle deposition velocities generally have very similar values in the two seasons.

- The particle deposition velocity v_t increases linearly with increasing friction velocity in both seasons. The relations are described by $v_{td}=(2.7u_*-0.2)\times10^{-3}$ in the dry season and $v_{tw}=2.5u_*\times10^{-3}$ in the wet season.

- Particle deposition velocities are low here in comparison to measurements made over boreal forests. The reason for this is probably dominance of accumulation mode particles in the Amazon boundary layer, both in the dry and wet season, and low wind speeds in the tropics compared to the midlatitudes. When considering the fact that wet deposition is a very important deposition process over tropical rain forests and adding the low particle deposition velocities found in this study, it can be stated that the relative contribution of dry deposition to total deposition of particles is much lower over tropical rain forests than over boreal forests, and instead comparable to many marine regions.

- Net particle deposition prevails in daytime both in the dry and wet season. This deposition flux is much larger in the dry season than in the wet season. Since daytime particle deposition velocities are similar in the two seasons, the much larger deposition flux in the dry season is a result of the higher dry season aerosol number concentration.

- In the dry season, nocturnal particle fluxes behave very similar to nocturnal CO_2 fluxes. Particle fluxes are very low in magnitude throughout the night but after sunrise upward particle fluxes appear. These appear before the nocturnal inversion has been defeated and are therefore not likely a result of entrainment. Nor does local pollution seem to be a likely explanation for these upward fluxes, since associated wind sectors have been excluded. Emission of natural biogenic particles from the forest, however, is a possible explanation. The upward flux appears

ACPD
9, 26881–26924, 2009

at the same time as the CO_2 emission flux. It is possible that particles are emitted throughout the night but stay within the canopy, which is decoupled from the atmosphere above, until turbulence mixes them up in the morning, similarly to what is observed for CO_2. It is also possible that they are emitted throughout the day, but then are masked by the larger deposition flux.

Hence, this study has shown that particle deposition velocities are very similar in the dry and wet season, which probably is due to rather similar size distributions in the two seasons, even though the total particle numbers are much higher in the dry season. However, it would be interesting to make the same dry/wet season comparison in the southern part of the Amazon rain forest where the impact from biomass burning on the dry season aerosol population is much larger.

The fact that net emission seems to prevail at nighttime in the dry season but not in the wet season is an indication that nocturnal particle emission from the forest may be favored by dry conditions. Upward particle fluxes with the magnitude of $0.5\times10^6\,m^{-2}\,s^{-1}$, like the observed morning upward flux in this study, would only increase the particle concentration with 18 particles per cm^3 and hour in a 100 m thick boundary layer. However, since nocturnal respiration is known to be underestimated by eddy covariance measurements, it is likely that also nocturnal particle emission is underestimated. The missing flux could be estimated by measuring the advection "out of the box" as been made for CO_2 by Tóta et al. (2008). Therefore in the future, horizontal gradients in aerosol concentrations and fluxes between plateaus and valleys should be examined.

Acknowledgements. We would like to thank the National Institute for Research in the Amazon (INPA) and the LBA infrastructure team for all help and support during this campaign. Paulo Artaxo acknowledges financial support from the CNPq/MCT Millennium Institute Program and FAPESP. We thank Paulo Henrique Oliveira (in memoriam) for support during the whole sampling campaign.

Swedish participation was provided by Swedish International Development Cooperation Agency (Sida/SAREC), the Swedish Research Council (VR) and from the 50th birthday of King Carl XVI Gustav Foundation for Science Technology and Environment. We also acknowledge Leif Bäcklin and Kai Rosman for technical assistance and the Bert Bolin centre for Climate Research School for financial support.

References

Ackerman, A. S., Toon, O. B., Stevens, D. E., Heymsfield, A. J., Ramanathan, V., and Welton, E. J.: Reduction of tropical cloudiness by soot, Science, 288, 1042–1047, 2000.

Ahlm, L., Nilsson, E. D., Krejci, R., Mårtensson, E. M., Vogt, M., and Artaxo, P.: Aerosol number fluxes over the Amazon rain forest during the wet season, Atmos. Chem. Phys. Discuss., 9, 17335–17383, 2009, http://www.atmos-chem-phys-discuss.net/9/17335/2009/.

Andreae, M. O., Browell, E. V., Garstang, M., Gregory, G. L., Harriss, R. C., Hill, G. F., Jacob, D. J., Pereira, M. C., Sachse, G. W., Setzer, A. W., Silva Dias, P. L., Talbot, R. W., Torres, A. L., and Wofsy, S. C.: Biomass-burning emissions and associated haze layers over Amazonia, J. Geophys. Res., 93, 1509–1527, 1988.

Andreae, M. O. and Merlet, P: Emission of trace gases and aerosols from biomass burning, Global Biogeochem. Cy., 15(4), 955–966, 2001.

Andreae, M. O., Artaxo, P., Fischer, H., Freitas, S. R., Grégoire, J. M., Hansel, A., Hoor, P., Kormann, R., Krejci, R., Lange, L., Lelieveld, J., Lindinger, W., Longo, K., Peters, W., de Reus, M., Scheeren, B., Silva Dias, M. A. F., Ström, J., van Velthoven, P. F. J., and Williams, J.: Transport of biomass burning smoke to the upper troposphere by deep convection in the equatorial region, Geophys. Res. Lett., 28(6), 951–954, 2001.

Andreae, M. O., Rosenfeld, D., Artaxo, P., Costa, A. A., Frank, G. P., Longo, K. M., and Silva-Dias, M. A. F.: Smoking rain clouds over the Amazon, Science, 303, 1337–1342, 2004.

Andreae, M. O. and Gelencsr, A.: Black carbon or brown carbon? The nature of light-absorbing carbonaceous aerosols, Atmos. Chem. Phys., 6, 3131–3148, 2006, http://www.atmos-chem-phys.net/6/3131/2006/.

Araújo, A. C., Kruijt, B., Nobre, A. D., Dolman, A. J., Maarten, J. W., Moors, E. J., and

Souza, J. S.: Nocturnal accumulation of CO_2 underneath a tropical forest canopy along a topographical gradient, Ecol. Appl., 18(6), 1406–1419, 2008.
Artaxo, P., Gerab, F., Yamasoe, M. A., and Martins, J. V.: Fine mode aerosol composition in three long term atmospheric monitoring sampling stations in the Amazon Basin, J. Geophys. Res., 99(D11), 22857–22868, 1994.
Artaxo, P. and Hansson, H.-C.: Size distribution of biogenic aerosol particles from the Amazon basin, Atmos. Environ., 29, 393–402, doi:10.1016/1352-2310(94)00178-N, 1995.
Artaxo, P., Fernandes, E. T., Martins, J. V., Yamasoe, M. A., Hobbs, P. V., Maenhaut, W., Longo, K. M., and Castanho, A.: Large-scale aerosol source apportionment in Amazonia, J. Geophys. Res., 103, 31837–31847, 1998.
Artaxo, P., Martins, J. V., Yamasoe, M. A., Procópio, A. S., Pauliquevis, T. M., Andreae, M. O., Guyon, P., Gatti, L. V., and Leal, A. M. C.: Physical and chemical properties of aerosols in the wet and dry season in Rondonia, Amazonia, J. Geophys. Res., 107, 8081, doi:10.1029/2001JD000666, 2002.
Aubinet, M., Heinesch, B., and Yernaux, M.: Horizontal and vertical CO_2 advection in a sloping forest, Bound.-Lay. Meteorol., 108(3), 397–417, 2003.
Bowman, D. M. J. S., Balch, J. K., Artaxo, P., Bond, W. J., Carlson, J. M., Cochrane, M. A., D'Antonio, C. M., DeFries, R. S., Doyle, J. C., Harrison, S. P., Johnston, F. H., Keeley, J. E., Krawchuk, M. A., Kull, C. A., Marston, J. B., Moritz, M. A., Prentice, I. C., Roos, C. I., Scott, A. C., Swetnam, T. W., van der Werf, G. R., and Pyne, S. J.: Fire in the Earth system, Science, 324, 481–484, doi:10.1126/science.1163886, 2009.
Buzorius, G., Rannik, Ü., Mäkelä, J. M., Keronen, P., Vesala,T., and Kulmala, M.: Vertical aerosol fluxes measured by the eddy covariance method and deposition of nucleation mode particles above a Scots pine forest in southern Finland, J. Geophys. Res., 105, 19905–19916, 2000.
Buzorius, G., Rannik, Ü., Nilsson, E. D., Vesala, T., and Kulmala, M.: Analysis of dry deposition velocity measurement techniques for particles smaller than 100 nm, J. Aerosol Sci. 34, 747–764, 2003.
Campos, J. G., Acevedo, O. C., Tóta, J., and Manzi, A. O.: On the temporal scale of the turbulent exchange of carbon dioxide and energy above a tropical rain forest in Amazonia, J. Geophys. Res., 11(4), D08124, doi:10.1029/2008JD011240, 2009.
Doebelin, E. O.: Measurement Systems, McGraw-Hill, New York, 1990.
Finnigan, J., Clement, R., Malhi, Y., Leuning, R., and Cleugh, H. A.: A re-evaluation of long-term

flux measurement techniques. Part I. Averaging and coordinate rotation, Bound.-Lay. Meteorol., 107, 1–48, 2003.
Finnigan, J.: An introduction to flux measurements in difficult conditions, Ecol. Appl., 18(6), 1340–1350, 2008
Fisch, G., Tóta, J., Machado, L. A. T., Dias, M., Lyra, R. F. D., Nobre, C. A., Dolman, A. J., and Gash, J. H. C.: The convective boundary layer over pasture and forest in Amazonia, Theor. Appl. Climatol., 78, 47–59, 2004.
Gaman, A., Rannik, Ü., Aalto, P., Pohja, T., Siivola, E., Kulmala, M., and Vesala T.: Relaxed eddy accumulation system for size resolved aerosol flux measurements, J. Atmos. Ocean. Tech., 21, 933–943, 2004.
Garstang, M., Ulanski, S., Greco, S., Scala, J., Swap, R., Fitzjarrald, D., Browell, E., Shipman, M., Connors, V., Harriss, R., and Talbot, R.: The Amazon boundary-layer experiment (ABLE 2B): a meteorological perspective, B. Am. Meteorol. Soc., 71, 19–31, 1990.
Goulden, M. L., Munger, J. W., Fan, S. M., Daube, B. C., and Wofsy, S. C.: Measurements of carbon sequestration by long-term eddy covariance: Methods and a critical evaluation of accuracy, Global Change Biol., 2, 169–182, 1996.
Graham, B., Guyon, P., Maenhaut, W., Taylor, P. E., Ebert, M., Matthias-Maser, S., Mayol-Bracero, O. L., Godoi, R., Artaxo, P., Meixner, F. X., Moura, M. A., Rocha, C. H., Grieken, R. V., Glovsky, M., Flagan, R., and Andreae, M. O.: Composition and diurnal variability of the natural Amazonian aerosol. J. Geophys. Res., 108(D24), 4765, doi:10.1029/2003JD004049, 2003.
Gunthe, S. S., King, S. M., Rose, D., Chen, Q., Roldin, P., Farmer, D. K., Jimenez, J. L., Artaxo, P., Andreae, M. O., Martin, S. T., and Pöschl, U.: Cloud condensation nuclei in pristine tropical rainforest air of Amazonia: size-resolved measurements and modeling of atmospheric aerosol composition and CCN activity, Atmos. Chem. Phys., 9, 7551–7575, 2009, http://www.atmos-chem-phys.net/9/7551/2009/.
Guyon, P., Graham, B., Beck, J., Boucher, O., Gerasopoulos, E., Mayol-Bracero, O. L., Roberts, G. C., Artaxo, P., and Andreae, M. O.: Physical properties and concentration of aerosol particles over the Amazon tropical forest during background and biomass burning conditions, Atmos. Chem. Phys., 3, 951–967, 2003, http://www.atmos-chem-phys.net/3/951/2003/.
Guyon, P., Graham, B., Roberts, G. C., Mayol-Bracero, O. L., Maenhaut, W., Artaxo, P., and Andreae, M. O.: In-canopy gradients, composition, sources, and optical properties of aerosol

over the Amazon forest, J. Geophys. Res., 108(D18), 4591, doi:10.1029/2003JD003465, 2003b.
Harris, P. P., Hunting, C., Cox, P. M., Gash, J. H. C., and Malhi, Y.: Effect of soil moisture on canopy conductance of Amazonian rainforest, Agr. Forest Meteorol., 122, 215–227, 2004.
Koren I., Martins, J. V., Remer, L. A., and Afargan, H.: Smoke invigoration versus inhibition of clouds over the Amazon, Science, 321, 946–949, 2008.
Kruijt, B., Malhi, Y., Lloyd, J., Nobre, A. D., Miranda, A. C., Pereira, M. G. P., Culf, A., and Grace, J.: Turbulence above and within two Amazon rainforest canopies, Bound.-Lay. Meteorol., 94, 297–311, 2000.
Lohmann, U., Stier, P., Hoose, C., Ferrachat, S., Kloster, S., Roeckner, E., and Zhang, J.: Cloud microphysics and aerosol indirect effects in the global climate model ECHAM5-HAM, Atmos. Chem. Phys., 7, 3425–3446, 2007, http://www.atmos-chem-phys.net/7/3425/2007/.
Marcolla, B., Cescatti, A., Montagnani, L., Manca, G., Kerschbaumer, G., and Minerbi, S.: Importance of advection in the atmospheric CO_2 exchanges of an alpine forest, Agr. Forest Meteorol., 130, 193–206, 2005.
Malhi, Y., Nobre, A. D., Grace, J., Kruijt, B., Pereira, M. G. P., Culf, A., and Scott, S.: Carbon dioxide transfer over a central Amazonian rain forest, J. Geophys. Res., 103, 31593–31612, 1998.
Martin, S. T., Andreae, M. O., Artaxo, P., Baumgardner, D., Chen, Q, Goldstein, A. H., Guenther, A., Heald, C. L., Mayol-Bracero, O. L., McMurry, P. H., Pauliquevis, T., Pöschl, U., Prather, K. A., Roberts, G. C., Saleska, S. R., Silva Dias, M. A., Spracklen, D. V., Swietlicki, E., and Trebs, I.: Sources and properties of amazonian aerosol particles, Rev. Geophys., in press, 2009.
Myneni, R. B., Yang, W., Nemani R. R., Hueted, A. R., Dickinsone, R. E., Knyazikhina, Y., Didan, K., Fue, R., Juárez, R. I. N., Saatchi, S. S., Hashimoto, H., Ichii, K., Shabanov, N. V., Tan, B., Ratana, P., Privette, J. L., Morisette, J. T., Vermotek, E. F., Roy, D. P., Wolfe, R. E., Friedl, M. A., Running, S. W., Votava, P., El-Saleous, N., Devadiga, S., Su, Y., and Salomonson, V.: Large seasonal swings in leaf area of Amazon rain forest, Proc. Natl. Acad. Sci. USA, 104, 4820–4823, 2007.
Oliveira, P. H. F., Artaxo, P., Pires, C., Lucca, S., Procopio, A., Holben, B., Schafer, J., Cardoso, L. F., Wofsy, S. C., and Rocha, H. R.: The effect of biomass burning aerosols and clouds on the CO_2 flux in Amazonia, Tellus B, 59, 338–349, 2007.

Pryor, S. C., Larsen, S. E., Sørensen, L. L., Barthelmie, R. J., Grönholm, T., Kulmala, M., Launiainen, S., Rannik, Ü., and Vesala, T.: Particle fluxes over forests: analyses of flux methods and functional dependencies, J. Geophys. Res., 112, D07205, doi:10.1029/2006JD008066, 2007.

Rannik, Ü., Vesala, T., and Keskinen, R.: On the damping of temperature fluctuations in a circular tube relevant to eddy covariance measurement technique, J. Geophys. Res., 102(D11), 12789–12794, 1997.

Reid, J. S., Koppmann, R., Eck, T. F., and Eleuterio, D. P.: A review of biomass burning emissions part II: intensive physical properties of biomass burning particles, Atmos. Chem. Phys., 5, 799–825, 2005, http://www.atmos-chem-phys.net/5/799/2005/.

Rissler, J., Swietlicki, E., Zhou, J., Roberts, G., Andreae, M. O., Gatti, L. V., and Artaxo, P.: Physical properties of the sub-micrometer aerosol over the Amazon rain forest during the wet-to-dry season transition – comparison of modeled and measured CCN concentrations, Atmos. Chem. Phys., 4, 2119–2143, 2004, http://www.atmos-chem-phys.net/4/2119/2004/.

Rissler, J., Vestin, A., Swietlicki, E., Fisch, G., Zhou, J., Artaxo, P., and Andreae, M. O.: Size distribution and hygroscopic properties of aerosol particles from dry-season biomass burning in Amazonia, Atmos. Chem. Phys., 6, 471–491, 2006, http://www.atmos-chem-phys.net/6/471/2006/.

Ruijgrok, W., Tieben, H., and Eisinga, P.: The dry deposition of particles to a forest canopy: a comparison of model and experimental results, Atmos. Environ., 31, 399–415, 1997.

Seinfeld, J. H. and Pandis, S. N.: Atmospheric Chemistry and Physics, John Wiley & Sons, 1998.

Slinn, W. G. N.: Predictions for particle deposition to vegetative canopies, Atmos. Environ., 16, 1785–1794, 1982.

Stull, R. B.: An Introduction to Boundary Layer Meteorology, Kluwer Academic Publishers, The Netherlands, 1988.

Tóta, J., Fitzjarrald, D. R., Staebler, R. M., Sakai, R. K., Moraes, O. M. M., Acevedo, O. C., Wofsy, S. C., and Manzi, A. O.: Amazon rain forest subcanopy flow and the carbon budget: Santarém LBA-ECO site, J. Geophys. Res., 113, G00B02, doi:10.1029/2007JG000597, 2008.

Webb, E. K., Pearman, G. I., and Leuning, R.: Correction of flux measurements for density

effects due to heat and water vapour transfer, Q. J. Roy. Meteorol. Soc., 106, 85–100, 1980.
Wesely, M. L., Cook, D. R., Hart, R. L., and Speer, R. E.: Measurements and parameterization of particular sulfur dry deposition over grass, J. Geophys. Res., 90, 2131–2143, 1985.
Zhang, L. and Vet, R.: A review of current knowledge concerning size-dependent aerosol removal, China Particuology, 4, 272–282, 2006.
Zhou, J. C., Swietlicki, E., Hansson, H. C., and Artaxo, P.: Submicrometer aerosol particle size distribution and hygroscopic growth measured in the Amazon rain forest during the wet season, J. Geophys. Res., 107, 8055, doi:10.1029/2000JD000203, 2002.

ACPD
9, 26881–26924, 2009

Table 1. Average conditions for critical parameters of measurements in the dry season. The±range after the mean value is the standard deviation and the numbers after the median are 10 and 90 percentiles. The average diurnal maximum and minimum have been calculated by taking the median value of all diurnal maxima and minima throughout the campaign. The numbers within the brackets in the max and min columns are 10 and 90 percentiles.

	Mean	Median	Diurnal max	Diurnal min
Temperature (°C)	26.4±3.0	26.0 (22.3, 28.9)	30.8 (28.9, 32.2)	22.9 (21.9, 23.9)
Relative humidity (%)	74.6±14.6	76.2 (52.8, 92.8)	93.4 (82.9, 96.1)	52.0 (44.8, 67.5)
Rain amount per day (mm)	2.8±5.9	0.2 (0, 10.1)	–	–
Photosynthetic active radiation ($W\,m^{-2}$)	130.6±179.7	3.4 (0, 433.9)	540 (434, 603)	0
Sensible heat flux ($W\,m^{-2}$)	19.9±44.4	–0.2 (–9.2, 91.5)	146.9 (80.3, 196.8)	–24.6 (–60.8, –10.0)
Water vapor molar density ($mmol\,m^{-3}$)	1242±125	1268 (1098, 1363)	1359 (1306, 1433)	1046 (628, 1190)
Latent heat flux ($W\,m^{-2}$)	90.7±144.1	11.9 (–2.2, 312.9)	429 (209, 527)	–9.6 (–106.4, –2.0)
Wind speed ($m\,s^{-1}$)	2.2± 0.9	2.1 (1.1, 3.3)	4.0 (3.2, 5.3)	0.7 (0.3, 1.4)
Friction Velocity ($m\,s^{-1}$)	0.19±0.17	0.14 (0.03, 0.46)	0.59 (0.37, 0.72)	0.011 (0.006, 0.026)
Inverted Obukhov length $1/L$ (m^{-1})	3.5±112.2	0.01 (–0.07, 0.24)	1.87 (0.47, 29.15)	–0.76 (–22.31, –0.06)
CO_2 molar density (ppm)	368±18	362 (353, 388)	401 (383, 467)	352 (345, 356)
CO_2 flux ($\mu mol\,m^{-2}\,s^{-1}$)	–1.46±6.32	0.09 (–11.05, 5.14)	11.1 (7.1, 19.5)	–15.0 (–19.0, –7.3)
Particle number concentration (cm^{-3})	1513±721	1352 (869, 2292)	2388 (1247, 4172)	982 (513, 1363)
Particle number flux ($10^6\,m^{-2}\,s^{-1}$)	–0.45±3.89	–0.20 (–2.66, 1.72)	4.11 (0.91, 16.6)	–5.14 (–24.79, –1.71)
BC_e concentration ($ng\,m^{-3}$)	259±115	245 (141, 375)	453 (250, 868)	146 (53, 202)

ACPD
9, 26881–26924, 2009

Table 2. Average conditions for critical parameters of measurements in the wet season. The±range after the mean value is the standard deviation and the numbers after the median are 10 and 90 percentiles. The average diurnal maximum and minimum have been calculated by taking the median value of all diurnal maxima and minima throughout the campaign. The numbers within the brackets in the max and min columns are 10 and 90 percentiles.

	Mean	Median	Diurnal max	Diurnal min
Temperature (°C)	24.6±2.3	24.0 (22.2, 28.2)	28.9 (26.3, 31.0)	22.2 (21.6, 23.1)
Relative humidity (%)	86.4±10.6	90.7 (69.2, 95.9)	96.0 (94.7, 96.5)	66.1 (54.6, 78.6)
Rain amount per day (mm)	10.8±12.8	5.6 (0.2, 29.1)	–	–
Photosynthetic active radiation ($W\,m^{-2}$)	84.6±129.7	1.5 (0, 303.6)	455 (275, 537)	0
Sensible heat flux ($W\,m^{-2}$)	14.4±47.2	–0.7 (–11.7, 77.3)	142.7 (36.0, 230.6)	–26.7 (–102.6, –10.2)
Water vapor molar density ($mmol\,m^{-3}$)	1120±170	1140 (970, 1250)	1246 (1160, 1606)	834 (275, 1150)
Latent heat flux ($W\,m^{-2}$)	71.4±133.1	11.5 (–2.2, 254.8)	368 (166, 489)	–23.1 (–116.2, –0.35)
Wind speed ($m\,s^{-1}$)	2.0±0.9	1.9 (0.9, 3.0)	3.6 (2.7, 4.8)	0.4 (0.2, 1.2)
Friction Velocity ($m\,s^{-1}$)	0.21±0.16	0.18 (0.04, 0.42)	0.52 (0.35, 0.77)	0.018 (0.008 , 0.063)
Inverted Obukhov length $1/L$ (m^{-1})	0.03±0.94	0.01 (–0.05, 0.11)	0.76 (0.05, 6.05)	–0.31 (–6.2, –0.01)
CO_2 molar density (ppm)	392±41	384 (366, 422)	430 (398, 540)	364 (349, 372)
CO_2 flux ($\mu mol\,m^{-2}\,s^{-1}$)	–1.38±7.37	0.47 (–13.15, 6.06)	11.3 (4.2, 17.3)	–17.6 (–19.7, –11.2)
Particle number concentration (cm^{-3})	682±780	466 (243, 1260)	853 (445, 5338)	263 (133, 458)
Particle number flux ($10^6\,m^{-2}\,s^{-1}$)	–0.32±3.50	–0.10 (–1.44, 1.03)	1.70 (0.40, 14.3)	–2.41 (–20.2, –0.51)
BC_e concentration ($ng\,m^{-3}$)	80±45	69 (36, 140)	131 (77, 263)	(21.4, 64.1)

ACPD
9, 26881–26924, 2009

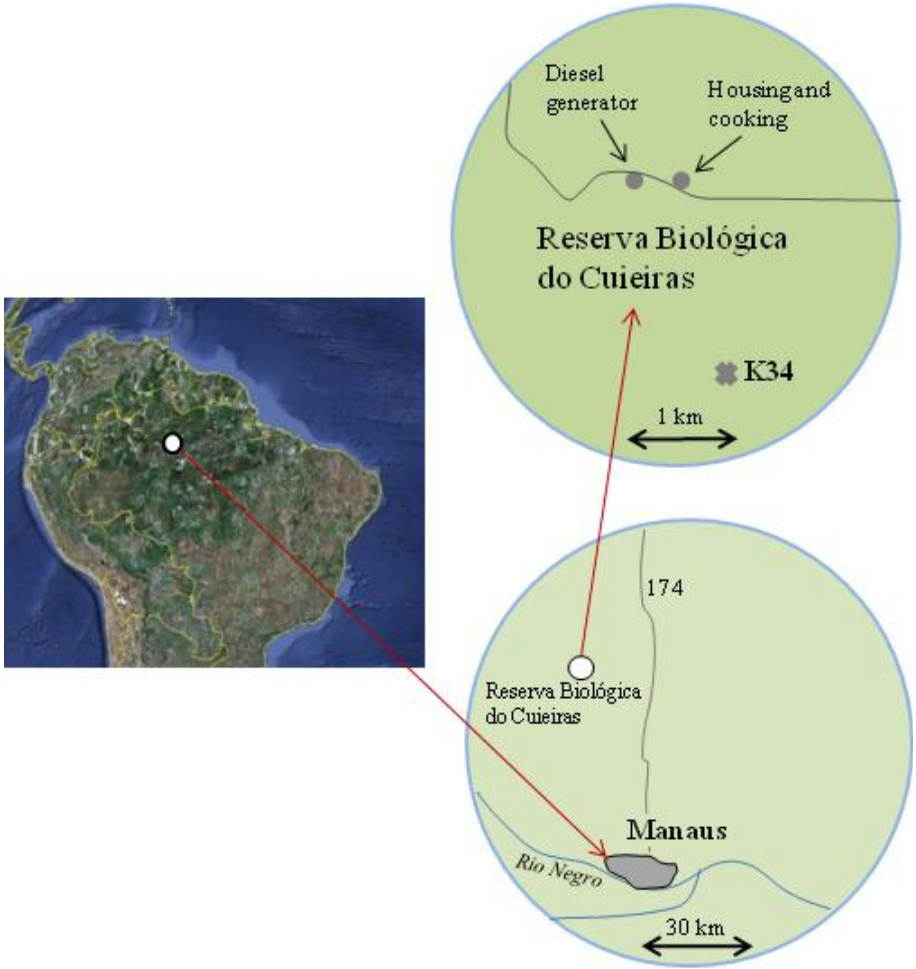

Fig. 1. Overview map of the measurement site in the Reserva Biológica do Cuieiras. The map over Northern South America to the left is taken from Google Earth.

ACPD
9, 26881–26924, 2009

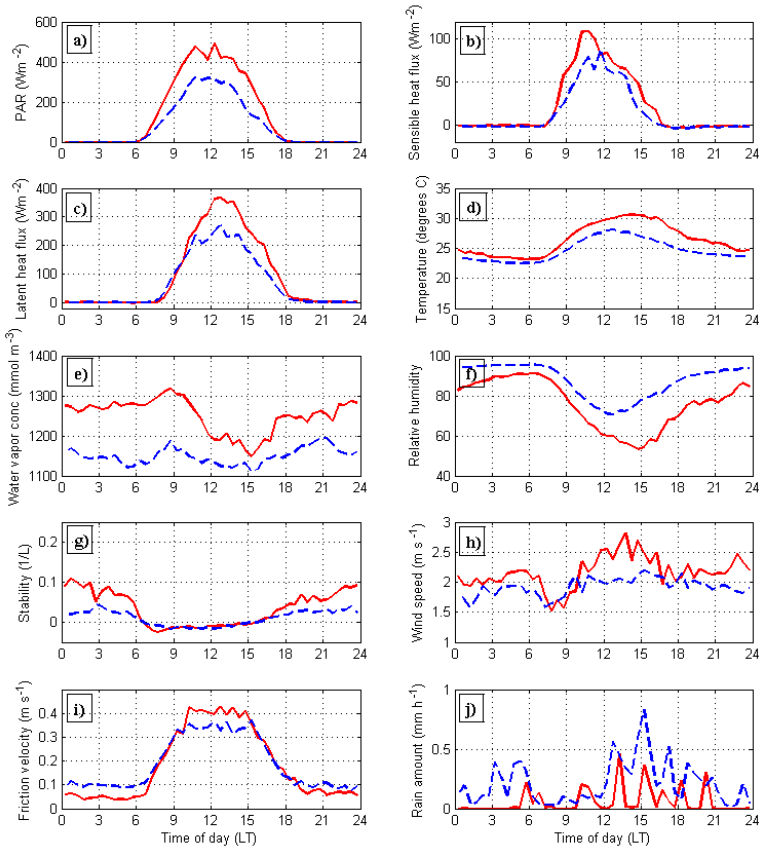

Fig. 2. Meteorological parameters measured at the top of the K34 tower. Solid red lines represent dry season and dashed blue lines represent wet season for **(a)** photosynthetic active radiation (PAR), **(b)** sensible heat flux, **(c)** latent heat flux, **(d)** temperature, **(e)** water vapor concentration **(f)** relative humidity, **(g)** stability (L^{-1}), **(h)** horizontal wind speed, **(i)** friction velocity, and **(j)** rain amounts.

ACPD
9, 26881–26924, 2009

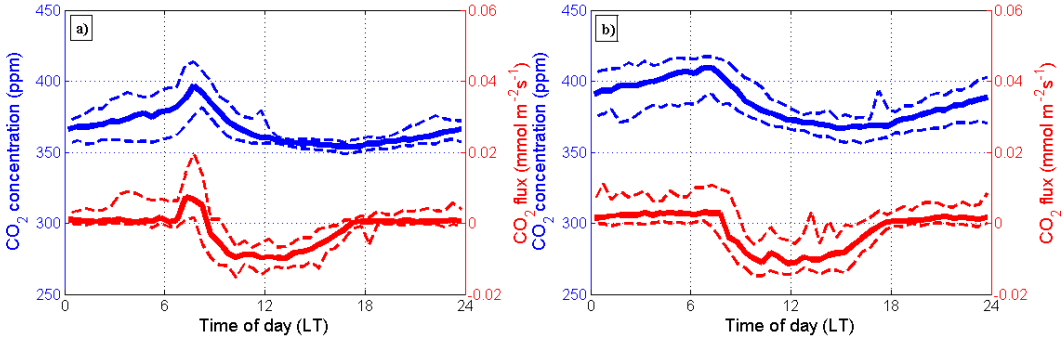

Fig. 3. Median diurnal cycles of CO_2 vertical flux (solid red lines) and concentration (solid blue lines) in the dry season **(a)** and wet season **(b)**. Dashed lines are 25 and 75 percentiles.

ACPD
9, 26881–26924, 2009

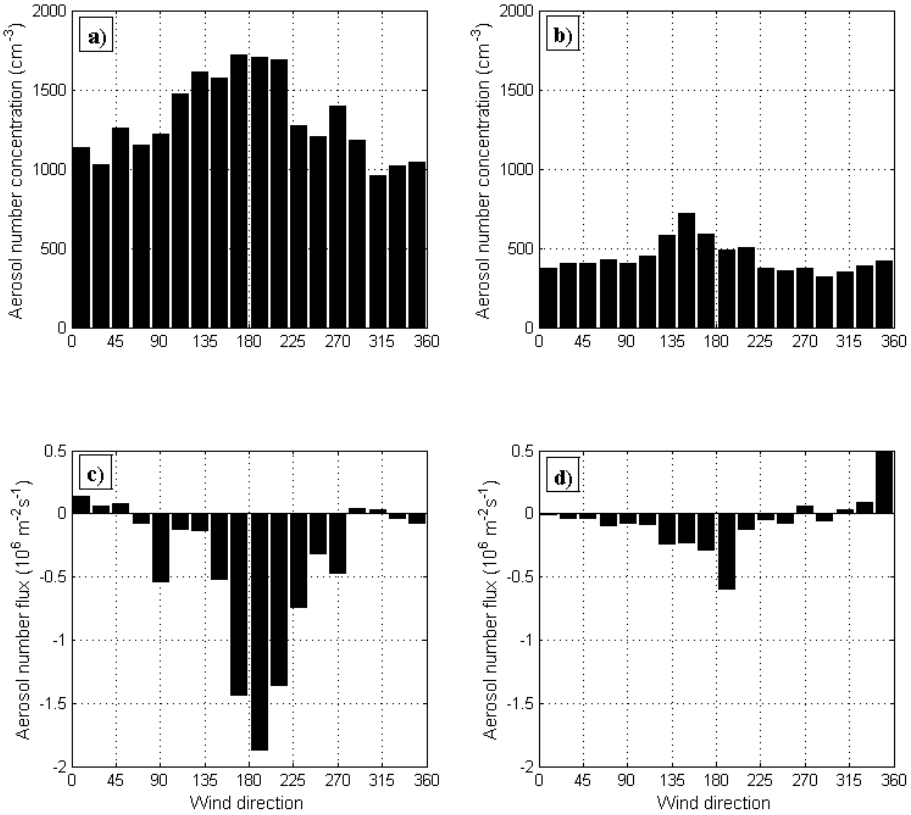

Fig. 4. Dependence on wind direction for the aerosol number concentration in the dry **(a)** and wet **(b)** season and for the aerosol number flux in the dry **(c)** and wet season **(d)**.

ACPD

9, 26881–26924, 2009

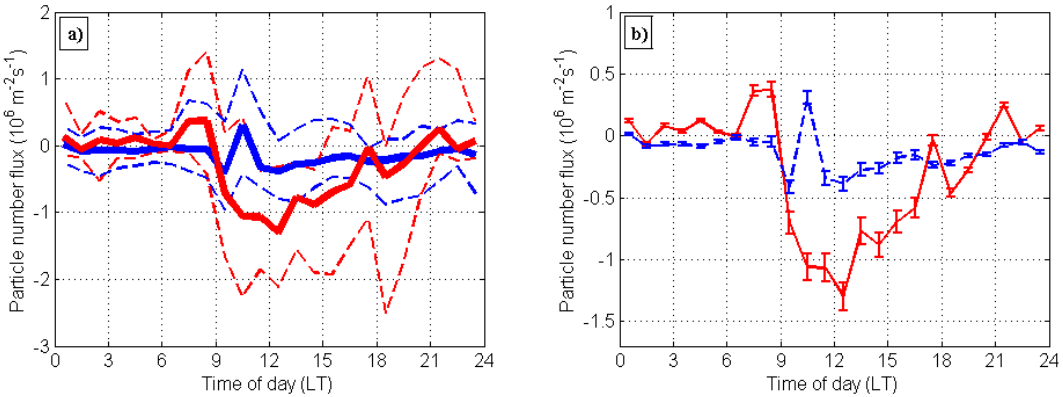

Fig. 5. **(a)** Median diurnal cycles of particle flux (solid lines) in the dry season (red) and wet season (blue). Dashed lines are 25 and 75 percentiles. **(b)** Median diurnal cycles of particle flux in the dry season (solid red line) and wet season (dashed blue line). Error bars represent median counting errors.

ACPD
9, 26881–26924, 2009

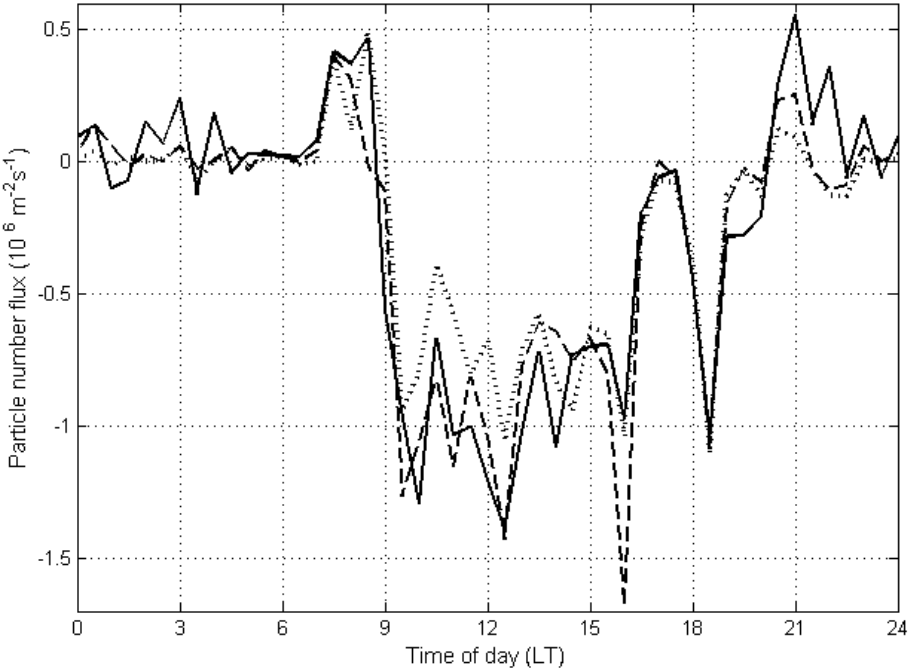

Fig. 6. Median diurnal cycles of the dry season aerosol number flux rotated and de-trended over 30 min (solid line), 10 min (dashed line) and 3 min (dotted line).

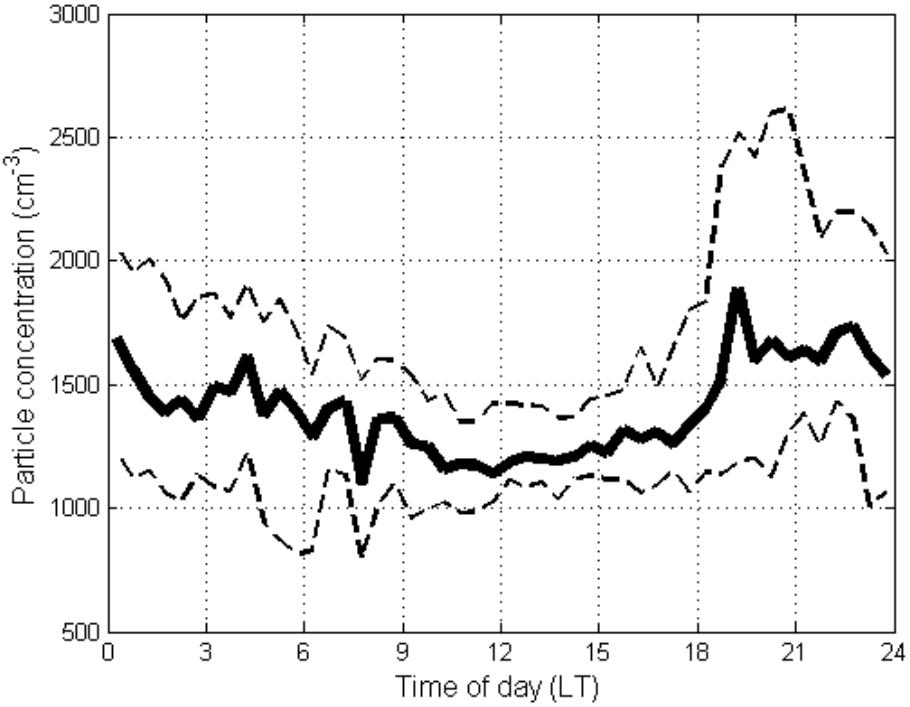

Fig. 7. Median diurnal cycle of the dry season aerosol number concentration (solid line) with 25 and 75 percentiles (dashed lines).

ACPD

9, 26881–26924, 2009

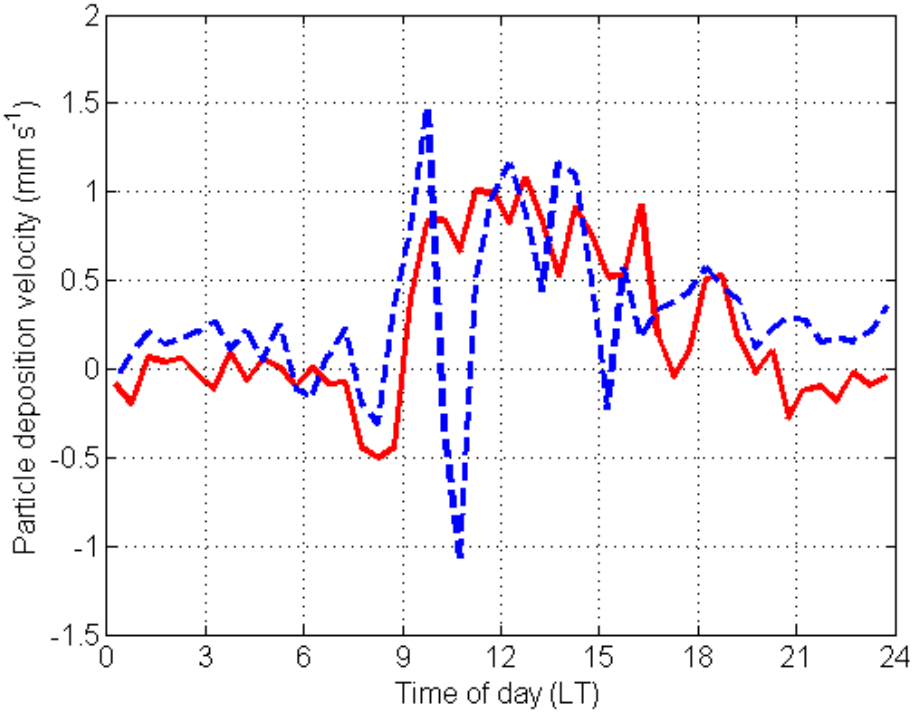

Fig. 8. Median diurnal cycles of particle deposition velocities in the dry (solid line) and wet (dashed line) season.

ACPD
9, 26881–26924, 2009

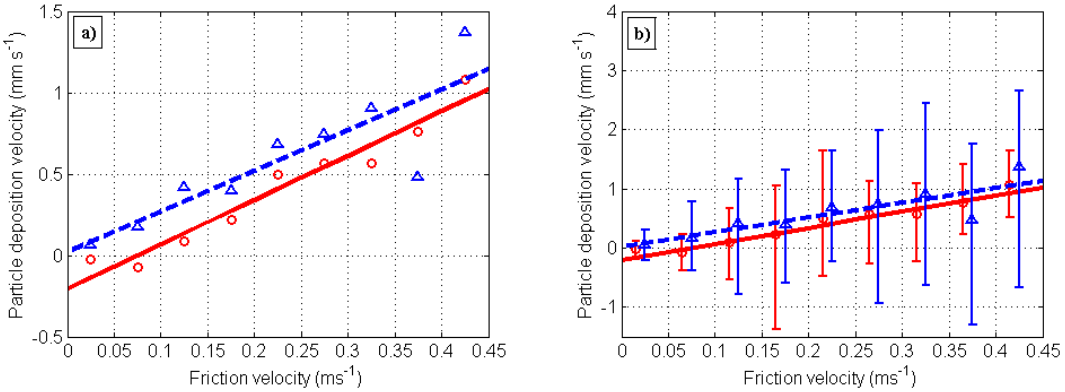

Fig. 9. **(a)** Medians of the particle deposition velocity over constant friction velocity intervals in the dry (red circles) and wet (blue triangles) season and linearly fitted curves to the dry (solid red line) and wet (dashed blue line) season data. **(b)** shows same as **(a)** with 25 and 75 percentiles included.

ACPD
9, 26881–26924, 2009

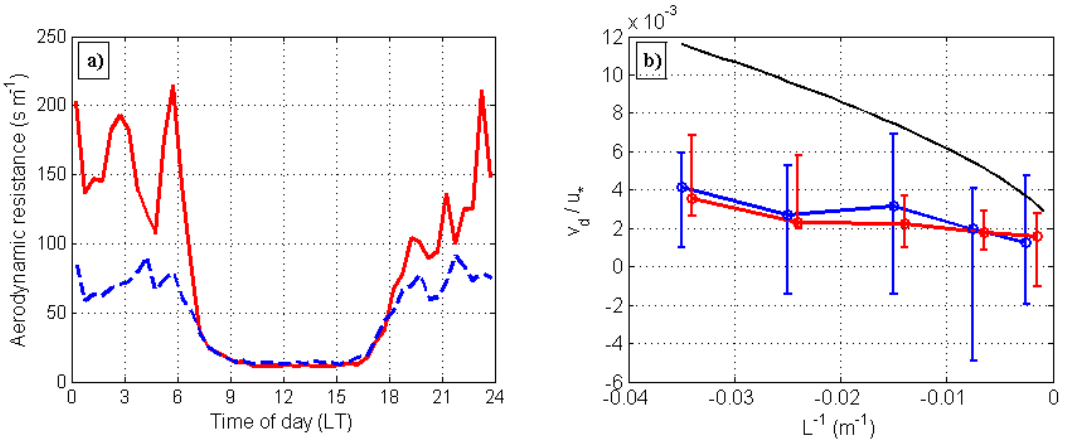

Fig. 10. **(a)** Median diurnal cycle of aerodynamic resistance in the dry season (solid red line) and wet season (dashed blue line). **(b)** v_d/u_* dependence on the inverted Obukhov length L^{-1} in the dry (red) and wet (blue) season with error bars corresponding to 25 and 75 percentiles. The black curve describes the unstable case of Eq. (8).

ACPD
9, 26881–26924, 2009